Korean Chem. Eng. Res., 53(5), 576-583 (2015)
http://dx.doi.org/10.9713/kcer.2015.53.5.576
PISSN 0304-128X, EISSN 2233-9558

Cempedak Durian (*Artocarpus sp.*) Peel as a Biosorbent for the Removal of Toxic Methyl Violet 2B from Aqueous Solution

Muhammad Khairud Dahri†, Hei Ing Chieng, Linda B. L. Lim, Namal Priyantha*, and Chan Chin Mei**

Department of Chemistry, Faculty of Science, Universiti Brunei Darussalam, Jalan Tungku Link, Gadong, Brunei Darussalam
**Department of Chemistry, Faculty of Science, University of Peradeniya, Peradeniya, Sri Lanka*
***Postgraduate Institute of Science, University of Peradeniya, Peradeniya, Sri Lanka*
(Received 24 December 2014; Received in revised form 27 January 2015; accepted 3 February 2015)

Abstract – This paper aims to investigate the potential use of cempedak durian peel (CDP) from Negara Brunei Darussalam, which is low-cost, locally available, eco-friendly and highly efficient to remove methyl violet (MV) dye from aqueous solutions. The time required for equilibrium to be reached is 2.0 h with no adjustment of pH necessary. FTIR analysis was indicative of the involvement of -COOH and C=O functional groups in adsorption process. The Langmuir model provided the best fit with maximum adsorption capacity of 0.606 mmol g^{-1}. Thermodynamics data indicate that the adsorption is spontaneous, feasible and endothermic in nature. Best regeneration of CDP's adsorption ability is achieved by base solution, showing about 95% removal efficiency of MV even after 5 cycles, indicating that CDP can be regenerated and reused. This, together with its high adsorption capacity, makes CDP a potential adsorbent for the removal of MV in wastewater.

Key words: Adsorption, Low-Cost Biosorbent, Water Remediation, Methyl Violet Dye, *Artocarpus*, Isotherms

1. Introduction

Due to their ease of production, stability and large range of colour, synthetic dyes have replaced the use of natural dyes in cosmetic, food, textile and leather industries, and subsequently, thousand tons of dye wastewater are produced annually[1]. Disposal of wastewater containing dyes destroy the esthetic nature of the water, and owing to their stable and synthetic nature, many dyes are usually resistant to biodegradation and furthermore their presence in water would interfere with light penetration and photosynthesis[2]. Untreated disposal of such wastewater can also affect humans as the dyes can bioaccumulate and goes up the food chain. Water bodies contaminated with dyes would exhibit low biological oxygen demand (BOD), high chemical oxygen demand (COD) and high amount of dissolved solid[3].

Chemical coagulation, ion exchange, reverse osmosis, chemical precipitation and oxidation are amongst the current methods used in order to remove/eliminate pollutants, such as dyes and heavy metals. However, they have certain limitations, such as formation of toxic by-products, high-cost, high reagent use and ineffective in removing pollutants at low levels[4]. Adsorption treatment utilizing commercial activated carbon, although effective, is associated with high-cost[5]. This leads to research on alternative, low-cost materials to substitute commercial activated carbon. Some low-cost adsorbents still include pine needle[6], peat[7-10], yeast[11], clay[12], duckweed[13], bacteria[14,15], fruit wastes[16,17], plant wastes[18,19] and algae [20,21], most of which are abundant and do not produce toxic by-products.

Methyl violet 2B (MV) dye ($C_{24}H_{28}N_3Cl$), whose structure is shown in Fig. 1, is also known as Basic violet 1. It is a dark green powder which produces intense violet coloured aqueous solution. MV is a multi-functional material: it is used for dyeing materials such as cotton, silk, paper, bamboo, weed, straw and leather; it is the active ingredient in Gram's biological stain for bacterial classification; it is a pH indicator which changes colour from yellow at low pH to bluish violet at high pH[22]. It is reported that the dye could hinder the growth of bacteria and photosynthesis of aquatic plants[23,24]. It could also be harmful by ingestion, inhaled and skin contact and long term exposure can cause eye and skin damages[23] and was reported to be potentially carcinogenic[25]. Thus, it is important for MV to be removed from industrial wastewater before it is discharged into the environment.

This paper aims to use Cempedak durian (*Artocarpus sp.*) peel (CDP) to remove MV from aqueous solution. Cempedak durian is one of the hybrids of *Artocarpus heterophyllus* (jackfruit) and *Artocarpus cempedan* (cempedak). It is less commonly known as it is grown mainly in the Borneo Island. As its name suggests, the texture and smell of the flesh closely resemble that of durian. Generally, more than 50% of *Artocarpus* fruits, e.g. skin and core, are inedible and are discarded as wastes[26,27]. Our research group has shown that *Artocarpus* fruit wastes are effective low-cost biosorbents for the removal of dyes and heavy metals[28-30]. As an extension, we aim to evaluate the use of CDP for the removal of MV as to date there has been no litera-

† To whom correspondence should be addressed.
E-mail: kiddri86@hotmail.com

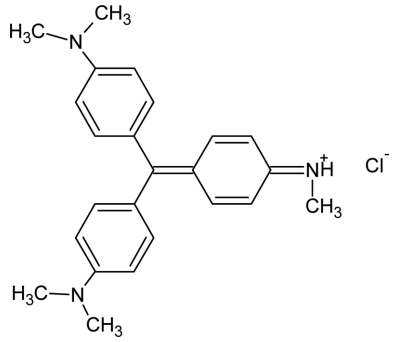

Fig. 1. Molecular structure of Methyl violet 2B.

ture report on the use of CDP as a biosorbent. Key parameters such as contact time, pH, temperature and ionic strength, are studied together with its characterization. Equilibrium adsorption isotherms, thermodynamics, kinetics and regeneration experiments are investigated to provide insight into the compatibility of the sample to be used as an effective biosorbent for the removal of MV.

2. Materials and Methods

2-1. Materials

Cempedak durian fruit was purchased from the local market and the peel of the fruit was separated and dried in oven at 85 °C until a constant mass was obtained. The dried cempedak durian peel (CDP) was then blended and sieved to obtain particles of diameter ranging from 355 μm to 850 μm.

2-2. Chemicals and reagents

Methyl violet 2B (80%) and potassium nitrate (99%) were purchased from Sigma-Aldrich. The solution pH was adjusted using NaOH (Univar) and HNO_3 (AnalaR). Spectroscopic grade KBr was used for FTIR analysis. Double distilled water was used throughout this study. Stock solution was prepared by dissolving appropriate amount of MV in double distilled water. Other concentrations of the dye were obtained by dilution of the stock solution. All reagents were used without further purification.

2-3. Instrumentation

Jenway 6320D spectrophotometer (UV-Vis) was used to measure the absorbance of MV at 584 nm for its quantification. Shimadzu IR Prestige-21 spectrophotometer was used for characterization of the functional groups present in CDP. The elemental composition (C, H, N and S) was determined using the Thermo Scientific Flash 2000 Organic Elemental Analyzer, while X-ray fluorescence (XRF) PANalyticalAxios^{max} instrument was used for other elemental analysis of CDP and MV-loaded CDP. The morphological analysis of CDP was performed using scanning electron microscope (SEM) model JEOL JSM-5800LV (Japan). Gerhardt soxtherm, Gerhardt Kjeldatherm and Gerhardt fibretherm were used for fat, protein and fat analysis, respectively.

2-4. Characterisation

Dried CDP was analysed for its fibre, fat and protein contents. The point of zero charge (pH_{pzc}) was determined by mixing 0.040 g of CDP with 20.0 mL of 0.10 M KNO_3, and the pH of the mixture was adjusted from 2 to 10. After 24 h agitation, the mixtures were filtered and the final pH was measured. The value of pH_{pzc} was calculated from the curve that intersects the X-axis of the plot of ΔpH versus pH_i (initial pH)[31].

2-5. Batch experimental procedure

Batch experiments were carried out by mixing 20.0 mL of known concentration of dye solution with 0.040 g of CDP (mass to volume ratio = 1:500) in clean 125 mL conical flask. The mixtures were then agitated on an orbital shaker at ambient temperature (25±1) °C at 250 rpm with the exception for thermodynamic experiments.

Experimental parameters, such as effect of contact time (5~240 min), effect of medium pH (3~10), effect of initial concentration (10~1,000 mg L^{-1}), ionic strength (0.1~0.8 M KNO_3) and effect of temperature (20~70 °C) were changed one parameter at a time, while other parameters being kept constant, and the extent of adsorption in each experiment was determined using the following relationships.

The amount of dye adsorbed per gram of CDP, q_e (mmol g^{-1}), was calculated using:

$$q_e = \frac{(C_i - C_e)V}{Mm} \quad (1)$$

where C_i is the initial dye concentration (mg L^{-1}), C_e is the equilibrium dye concentration (mg L^{-1}), M is the dye molecular mass (mol g^{-1}) V is the volume of MV solution used (L), and m is the mass of CDP used (g). The percentage removal of the dye is represented by:

$$\text{Percentage removal} = \frac{(C_i - C_e) \times 100\%}{C_i} \quad (2)$$

2-6. Regeneration of CDP

Regeneration of CDP's adsorption capacity was studied using 3 different washing solutions: double distilled water, 0.1 M HNO_3 and 0.1 M NaOH. For this purpose, 0.5 g of CDP was treated with 100 mg L^{-1} MV using the same optimized conditions described in Section *2.5*. After treatment, the MV-loaded CDP was thoroughly washed with double distilled water and dried in an oven for 24 h at 85 °C as preparation for the regeneration study. The dried samples were then divided and treated with different washing solutions mentioned. After agitating MV-loaded CDP with each washing solution, double distilled water was used to thoroughly wash the sample to remove any remaining dye, acid or base before drying in the oven for 24 at 85 °C. This was considered as one cycle and the experiment was done in five cycles.

3. Results and Discussion

3-1. Characterisation of CDP

Cempedak durian fruit comprises of peel (45.7%), core (12.8%)

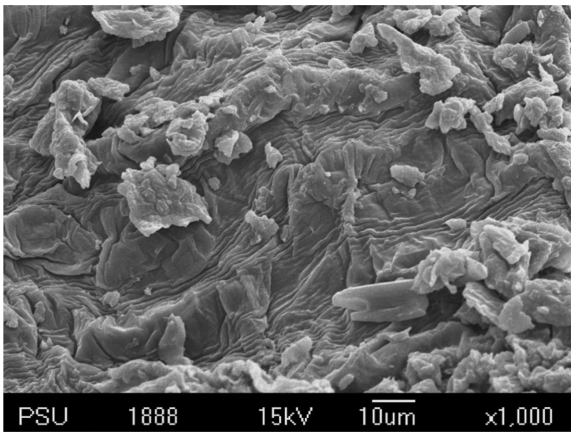

Fig. 2. SEM image of CDP surface at x1,000 magnification.

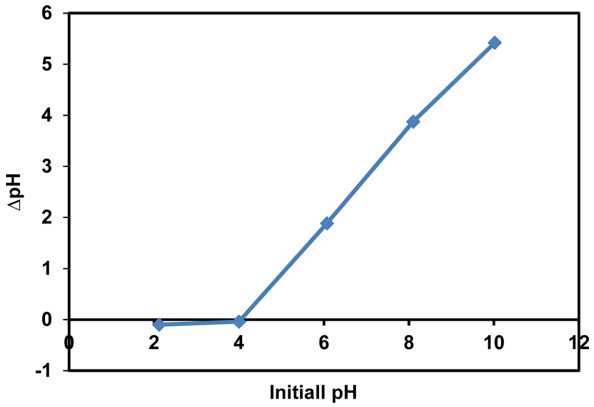

Fig. 4. Point of zero charge plot of CDP (CDP mass = 0.04 g; [KNO_3] = 0.1 M; volume of KNO_3 = 20.0 mL; agitation speed = 250 rpm; agitation time = 24 h).

and flesh and seed (24.1%). The peel, which is inedible and normally discarded as waste, consists the highest composition in the fruit. Hence, it would be more beneficial if the peel could be utilized as an adsorbent for the removal of dyes. CDP contained 19.7% crude fiber, 4.83% crude protein and 2.50% crude fat. The elemental compositions of CDP are 42.9% C, 5.3% H, 1.2% N and <0.5% for S. According to XRF analyses, before and after adsorption of MV on CDP, the levels of K (35%), Mg (18%) and Ca (3%) have decreased upon treatment of MV to 16%, 0.5% and 1%, respectively. This observation suggests an ion-exchange behaviour owing to the positive charge of the adsorbate molecules. The morphological analysis using SEM shows that the surface of CDP is irregular (Fig. 2) which might provide large surface area for adsorption.

FTIR spectrum of both untreated and MV-treated CDP is shown in Fig. 3. The broad peak at 3,385 cm^{-1} represent OH and NH stretching vibration whereas peak at 1,633 cm^{-1} represent C=C group. NH bending vibration is seen at 1,519 cm^{-1} and the C-N bond is present at 1,373 cm^{-1}. After treatment with MV, the peaks of C=C, NH and C-N were shifted to 1,589, 1,523 and 1,367 cm^{-1}, respectively. The resulting prominent shifts indicate that these functional groups might be involved in the adsorption of MV onto CDP's surface.

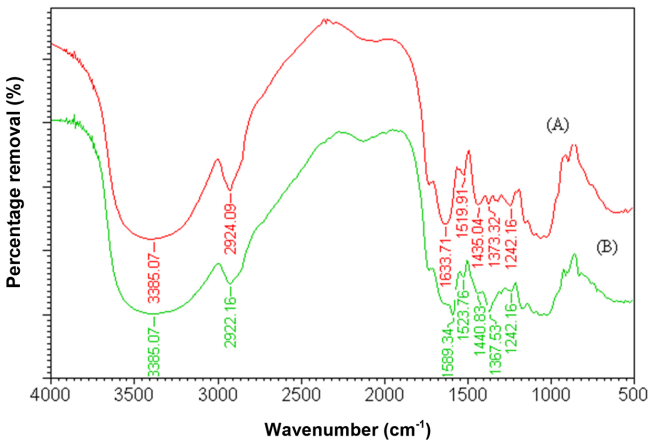

Fig. 3. FTIR spectra of (A) CDP and (B) MV-loaded CDP.

pH_{pzc} is the pH at which the surface has zero net charge (neutral) and this is an important and useful information in dealing with pH, one of the most important factors in adsorption processes. When pH > pH_{pzc}, acidic functional groups on the surface will dissociate and becomes predominantly negatively charged, while at pH < pH_{pzc}, the surface is associated with H^+ and becomes predominantly positively charged. Therefore, depending on the pH, the adsorption of charged ions or molecules, is favoured or suppressed due to the electrostatic interaction. The pH_{pzc} for CDP was determined as 4.01 as shown in Fig. 4.

3-2. Effect of contact time

Contact time is a useful parameter in designing economical wastewater treatment systems[32]. From Fig. 5, rapid increase in adsorption capacity, q_e, was observed within 30 min followed by saturation level after 60 min. The rapid increase was due to the availability of active sites on CDP for MV to interact with. Although the equilibrium was reached at 60 min, 120 min was selected as the optimal contact time to assure the complete equilibrium.

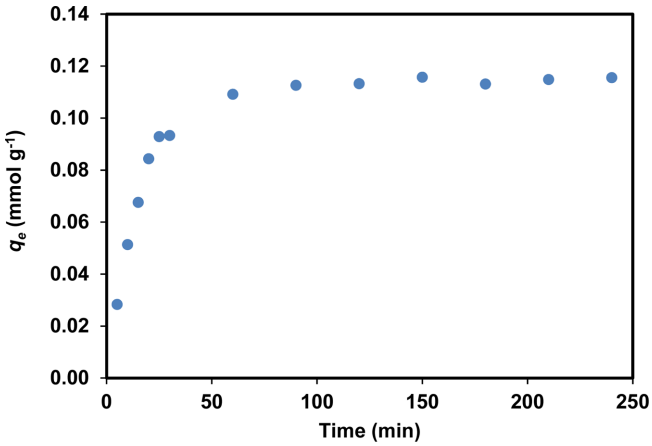

Fig. 5. The effect of contact time on removal of MV by CDP (CDP mass = 0.04 g; volume of MV = 20.0 mL; concentration of MV = 100 mg L^{-1}; agitation speed = 250 rpm; temperature = 25 °C).

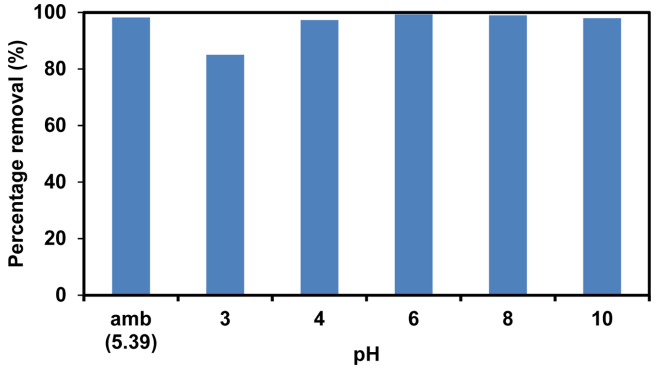

Fig. 6. Effect of different medium pH on the adsorption of MV onto CDP (CDP mass = 0.04 g; volume of MV = 20.0 mL; concentration of MV = 10 mg L^{-1}; agitation speed = 250 rpm; temperature = 25 °C).

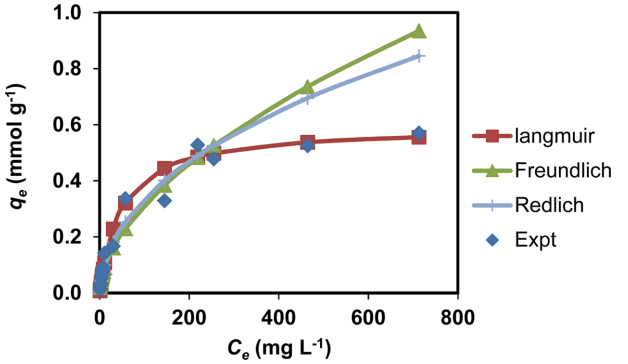

Fig. 7. Comparison of non-linear regression of experimental plot with Langmuir, Freundlich and Redlich-Peterson plots.

3-3. Effect of pH

The pH of solution is one of the important parameters in adsorption studies as pH will affect the adsorbent's surface charge and at the same time may influence the degree of ionization of dye. Figure 6 shows the effect of pH on the adsorption of 10 mg L^{-1} MV onto CDP. The pH of 3.0 has the lowest removal of about 85% as compared to the rest of the pHs with almost 100% removal. As MV becomes positively charged when dissolved in water (Fig. 1), the adsorption is favourable at pH higher than 4 as CDP pH_{pzc} is 4.01. At low pH, the positively charged surface of CDP would have electrostatic repulsion with MV. Above pH 4, negatively charged CDP sites increased thereby enhancing the adsorption of MV. In this paper, no pH adjustment was required as the ambient pH (5.39) has comparable removal value as those at higher pH.

It is noted that, despite pH 3 is lower than CDP's pH_{pzc}, the removal of MV was not severely affected. This shows that electrostatic interaction does not play major role in the adsorption process as pure reliance on such interaction would severely affect the removal ability of the adsorbent. Other forces such as hydrophobic interaction, ion-exchange and hydrogen bonding may work together alongside electrostatic interaction in the adsorption process. XRF results also support this claim as explained in Section 3-1.

3-4. Adsorption isotherm

Adsorption isotherm is crucial in the design of adsorption systems in wastewater treatment as it provides insight into interaction between the adsorbate and adsorbent. The equilibrium data obtained for MV onto CDP was fitted to three isotherm models i.e. the Langmuir[33], Freundlich[34] and Redlich-Peterson[35] models. The best fit model for the adsorption isotherm conducted in the range of 10~1,000 mg L^{-1} MV under optimized conditions was chosen based on the coefficient of determination (R^2) value, fitting of the non-linear regression isotherms (Fig. 7) and error analyses as shown in equations (3) to (6) for the average relative error (ARE), the sum of absolute error (EABS), the Marquart's percent standard deviation (MPSD) and the chi-square test (χ^2), respectively.

$$\text{ARE: } \frac{100}{p}\sum_{i=1}^{p}\left|\frac{q_{e,meas}-q_{e,calc}}{q_{e,meas}}\right|_i \tag{3}$$

$$\text{EABS: } \sum_{i=1}^{p}\left|q_{e,meas}-q_{e,calc}\right| \tag{4}$$

$$\text{MPSD: } 100\sqrt{\frac{1}{p-n}\sum_{i=1}^{p}\left(q_{e,meas}-q_{e,calc}\right)^2} \tag{5}$$

$$\chi^2\text{: } \sum_{i=1}^{p}\frac{\left(q_{e,meas}-q_{e,calc}\right)^2}{q_{e,meas}} \tag{6}$$

where $q_{e,meas}$ is the experimental value while $q_{e,calc}$ is the calculated value from the isotherm models, n is the number of parameter and p is the number of observations in the experiment. Smaller values of these error analysis indicates the better curve fitting[36].

The Langmuir isotherm assumes a monolayer adsorption onto the surface with a definite number of identical sites. The linearized form of the Langmuir is given by Eq. (7) as follows:

$$\frac{C_e}{q_e}=\frac{1}{b\,q_m}+\frac{C_e}{q_m} \tag{7}$$

The separation factor (R_L) is a dimensionless constant which is an important characteristic of the Langmuir model[37]. It is given by the following equation,

$$R_L=\frac{1}{(1+bC_o)} \tag{8}$$

where q_m is the maximum monolayer biosorption capacity of the adsorbent (mmol g^{-1}), b is the Langmuir biosorption constant (L mg^{-1}) which is related to the free energy of biosorption, and C_0 (mg L^{-1}) and C_e (mg L^{-1}) are the highest initial dye concentration and equilibrium dye concentration respectively. R_L indicates whether the isotherm is either unfavorable ($R_L > 1$), linear ($R_L = 1$), favorable ($0 < R_L < 1$), or irreversible ($R_L = 0$)[38].

The Freundlich isotherm model takes account of multilayer coverage where the dye is adsorbed on the dye saturated adsorbent surface. The linearized equation for the Freundlich is given by:

$$\ln q_e=\frac{1}{n_F}\ln C_e+\ln K_F \tag{9}$$

where K_F [mmol g^{-1} (L $mmol^{-1})^{1/n}$] is the adsorption capacity of

Table 1. Parameters calculated for the Langmuir, Freundlich and RP isotherm models

Langmuir		Freundlich		RP	
q_m (mmol g^{-1})	0.606 ± 0.018	K_F [mmol g^{-1} (L $mmol^{-1})^{1/n}$]	0.0240 ± 0.0004	K_R (L mg^{-1})	0.030 ± 0.010
b (L mg^{-1})	0.0210 ± 0.0002	n_F (-)	1.822 ± 0.043	β (-)	0.582 ± 0.020
R_L	0.0460 ± 0.0003			a_R (L mg^{-1})	0.563 ± 0.027
R^2	0.990 ± 0.003	R^2	0.9520 ± 0.0004	R^2	0.957 ± 0.005
ARE	15.821	ARE	23.071	ARE	16.573
EABS	0.360	EABS	0.938	EABS	0.770
MSPD	22.354	MSPD	31.483	MSPD	23.468
χ^2	0.085	χ^2	0.399	χ^2	0.249

the adsorbent while n_F(-), the Freundlich constant, gives indication of how favorable the adsorption process (adsorption intensity) is or surface heterogeneity.

The Redlich-Peterson (RP) isotherm model incorporates three parameters which may represent the adsorption process over a wide concentration range and can be applied either in homogeneous or heterogeneous systems due to its versatility[35]. The linearized form of the RP isotherm is as follows:

$$\ln\left[\frac{K_R C_e}{q_e} - 1\right] = \ln a_R + \beta \ln C_e \quad (10)$$

where K_R (L g^{-1}) and a_R (L mg^{-1}) are RP isotherm constants and β is an exponent.

The three isotherm models were compared in order to determine which best fits the experimental data. The values of R^2 (Table 1) of the three isotherm models were all above 0.95 which indicate the suitability of the models used with the experimental data; however, the Langmuir model has the highest R^2 value, close to unity, suggesting that this model is a better fit with the experimental data. The proximity of Langmuir non-linear regression plot with that of experimental data (Fig. 7) as well as the lower error analysis values (Table 1) as compared to the other two models provide further support for the Langmuir model to be accepted to describe the experimental data. Both values of R_L and n_F point toward favourable adsorption process of MV onto CDP. The maximum adsorption capacity, q_{max}, of CDP was determined as 0.606 mmol g^{-1} (238.7 mg g^{-1}). Compared to various absorbents as shown in Table 2, CDP showed a relatively high q_{max} which indicates that it has potential to be an adsorbent for the removal of MV from aqueous solution.

Table 2. Comparisons of q_m values with other adsorbents

Adsorbent	q_m (mg g^{-1})	Reference
Cempedak durian peel (CDP)	238.5	This work
Tarap peel	137.3	[28]
Duckweed	332.5	[13]
Casuarina equisetifolia needle	165.0	[6]
Orange peel	11.5	[39]
Banana peel	12.2	[39]
Pu-erh Tea powder (40 mesh)	278.0	[40]
Posidonia oceanic (L.) leaf	119.0	[41]
Almond shell	76.3	[42]

3-5. Adsorption kinetics

Kinetics studies provide information in understanding of the mechanism of adsorption processes. Movement of adsorbate from the bulk solution to the adsorbent's surface occurs in two steps: migration of adsorbate molecule to the external surface of adsorbent particles, molecular and pore diffusion may occur either singly or all together at once[43]. Four kinetics models namely the Lagergren 1st-order[44], pseudo-2nd-order[45], Weber-Morris intraparticle diffusion[46] and Boyd[47] models, whose equations are shown in (11) to (15), were used to describe the mechanism of the sorption process:

i) Lagergren 1st-order model,

$$\log(q_e - q_t) = \log q_e - \frac{t}{2.303} k_1 \quad (11)$$

ii) Pseudo-2nd-order,

$$\frac{t}{q_t} = \frac{1}{q_e^2 k_2} + \frac{t}{q_e} \quad (12)$$

iii) Weber and Morris intraparticle diffusion model,

$$q_t = k_3 t^{1/2} + C \quad (13)$$

iv) Boyd model,

$$B_t = -0.4977 - \ln(1 - F) \quad (14)$$

$$F = \frac{q_t}{q_e} \quad (15)$$

where q_t is the amount of adsorbate adsorbed per gram of adsorbent (mmol g^{-1}) at time t, k_1 is the pseudo-first-order rate constant (min^{-1}), t is the time shaken (min), k_2 is pseudo second order rate constant (g $mmol^{-1}$ min^{-1}), k_3 is the intraparticle diffusion rate constant (mmol g^{-1} $min^{-1/2}$) and C is the slope that represents the thickness of the boundary layer. F is the fraction of dye adsorbed at different time and B_t is a mathematical function of F.

The Lagergren 1st-order's parameters q_e and k_1 were obtained from the intercept and slope of the plot $\ln(q_e - q_t)$vs t respectively. Similarly, q_e and k_2 of pseudo-2nd-order were obtained from slope and intercept of the linear plot $\frac{t}{q_t}$ vs t, respectively as shown in Fig. 8. Table 3 shows the parameters obtained from plotting all four models. Comparing the R^2 values between the Lagergren 1st-order and pseudo-2nd-order, the latter has higher value than the former, indicating pseudo-2nd-order might be better fitted to the experimental data.

Table 3. The parameters of Lagergren 1st-order, pseudo-2nd-order, Weber - Morris intraparticle diffusion and Boyd models for adsorption of MV by CDP

Lagergren 1st-order		Pseudo-2nd-order		Intraparticle diffusion		Boyd	
$q_{e,exp}$ (mmol g^{-1})	0.1160 ± 0.0001	$q_{e,exp}$ (mmol g^{-1})	0.1160 ± 0.0001	k_{3A} (mmol g^{-1} $min^{-1/2}$)	0.0210 ± 0.0004	R^2	0.833 ± 0.032
$q_{e,cal}$ (mmol g^{-1})	0.043 ± 0.001	$q_{e,cal}$ (mmol g^{-1})	0.1210 ± 0.0002	C_A	- 0.016 ± 0.003	y intercept	0.499 ± 0.023
k_1 (min^{-1})	0.0160 ± 0.0002	k_2 (g $mmol^{-1}$ min^{-1})	0.800 ± 0.036	k_{3B} (mmol g^{-1} $min^{-1/2}$)	0.0010 ± 0.0001	Slope	0.0160 ± 0.0002
R^2	0.833 ± 0.032	R^2	0.999 ± 0.001	C_B	0.105 ± 0.001		

This is further confirmed by the similar q_e values between pseudo-2nd-order (0.121 mmol g^{-1}) and experimental data (0.116 mmol g^{-1}) than that of Lagergren 1st-order (0.043 mmol g^{-1}). Pseudo-2nd-order model is based on the assumption that chemisorption involving valency forces through sharing or exchange of electrons between adsorbent and adsorbate may be the rate-limiting step[45]. The deviation of calculated q_e of the Largergren 1st-order model from experimental value could be due to the inability of this model to describe entire range of adsorption time and limited only to the initial time range[48].

The adsorption process can be described by several steps: 1) transport in solution bulk 2) diffusion on the adsorbent's surface (film diffusion) 3) adsorbate transport occurs within the adsorbent's pores (particle diffusion) and 4) sorption and desorption within the particle and adsorbent's surface[49]. Generally, step 2 and step 3 are considered to be rate - limiting step as the other two steps occur rapidly. Weber - Morris intraparticle diffusion and Boyd models were used to describe the diffusion mechanism of the adsorption process as the previous kinetic models were not suitable to be used in describing the diffusion mechanism. Intraparticle diffusion mechanism is considered as rate-limiting step for the adsorption process when the linear plot of q_t versus $t^{1/2}$ passes through the origin[46]. In this study, the Weber-Morris intraparticle diffusion plot shown in Fig. 8C is not a linear line but instead is divided into two regions. The first linear region (A) is attributed to boundary layer diffusion while the second region (B) indicates intraparticle diffusion and chemical reaction[50]. However, none of these linear regions pass through origin according to the value of C_A and C_B (Fig. 8C and Table 3), indicating intraparticle diffusion is not the rate limiting step. The value *C* represents the boundary layer thickness whereby the larger the value, the greater is the boundary layer effect.

For Boyd model, plotting B_t against t should yield a straight line graph whereby if the line passes through the origin, the adsorption process might be controlled by particle diffusion and if it does not passes through the origin, the process might be controlled by film diffusion[47]. However, the plot does not pass through the origin (Table 3) which suggests that adsorption of MV onto CDP may be controlled by film diffusion.

3-6. Effect of ionic strength

Dye wastewater effluents can contain salt which may interfere with the adsorption process as ionic strength can influence the electrostatic interaction and hydrophobic-hydrophobic interaction[51].

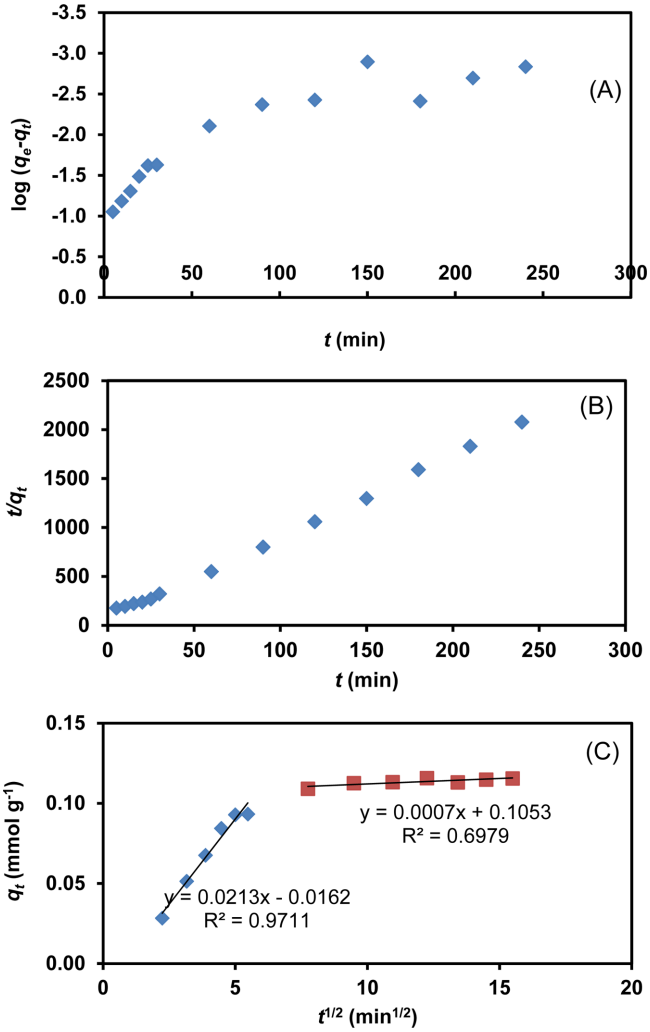

Fig. 8. Kinetics plots of (A) Lagergren 1st-order (B) Pseudo-2nd-order and (C) Weber - Morris intraparticle diffusion model.

Effect of KNO_3 on the adsorption process with concentrations ranging from 0.01 M to 0.80 M is shown in Fig. 9. It can be seen that, addition of 0.1 M of KNO_3 reduced the adsorption capacity of CDP by about 30%. Further decrease was oberved when higher concentration of the salt is introduced where the adsorption capacity is reduced by 50% in 0.8 M KNO_3.

The reduction upon addition of the salt may due to the electrostatic competition of K^+ with the cationic dye molecules[51,52]. The buildup of K^+ on the active site also created electrostatic repulsion between the adsorbent and the dye molecule thus lowering the dye adsorption. In theory, increase in ionic strength decreases the adsorption capac-

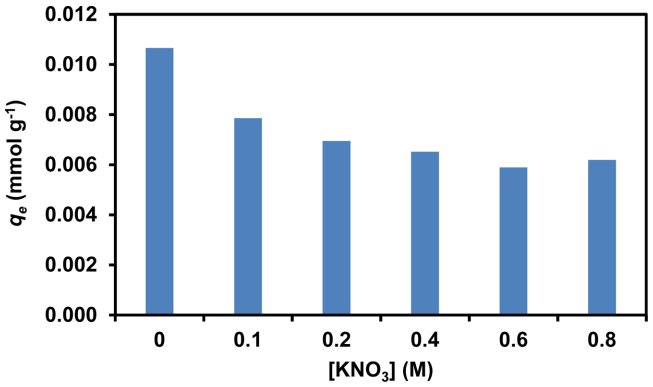

Fig. 9. Effect of different concentration of KNO_3 on the removal of MV by CDP (mass = 0.04 g; volume of MV = 20.0 mL; concentration of MV = 10 mg L^{-1}; agitation speed = 250 rpm; temperature = 25 °C).

ity when the electrostatic forces between the adsorbent and adsorbate are attractive while the adsorption capacity is increased when the electrostatic forces between them are repulsive in solution with increasing ionic strength[53]. The observation in this study is in agreement with the observations made in pH variation and in XRF studies where the cations have interfered with the adsorption of dye molecule.

3-7. Determination of thermodynamics parameters

Thermodynamics parameters such as the Gibbs free energy (ΔG^o), enthalpy (ΔH^o) and entropy (ΔS^o) were investigated by studying the sorption process at different temperatures (20, 40, 50, 60 and 70 °C). Van't Hoff equation was used to calculate these variables:

$$\Delta G^o = -RT\ln K \quad (16)$$

$$K = \frac{C_s}{C_e} \quad (17)$$

$$\Delta G^o = \Delta H^o - T\Delta S^o \quad (18)$$

$$\ln K = \frac{\Delta S^o}{R} - \frac{\Delta H^o}{RT} \quad (19)$$

where K is the distribution coefficient for adsorption, C_S is the equilibrium dye concentration on the CDP (mg L^{-1}), C_e is the equilibrium dye concentration in solution (mg L^{-1}), R is the gas constant (J K^{-1} mol^{-1}) and T is the temperature (K).

As seen in Table 4, the adsorption process becomes more spontaneous as the temperature increases indicated by ΔG^o being more negative as temperature increases. This is supported by the positive ΔH^o value which shows that the process is endothermic in nature.

Table 4. Thermodyamics parameters for the adsorption of MV onto CDP

Temperature (K)	ΔG^o (kJ mol^{-1})	ΔH^o (kJ mol^{-1})	ΔS^o (J mol^{-1} K^{-1})
298	-5.82		
313	-6.37		
323	-6.76	4.09	33.40
333	-7.15		
343	-7.24		

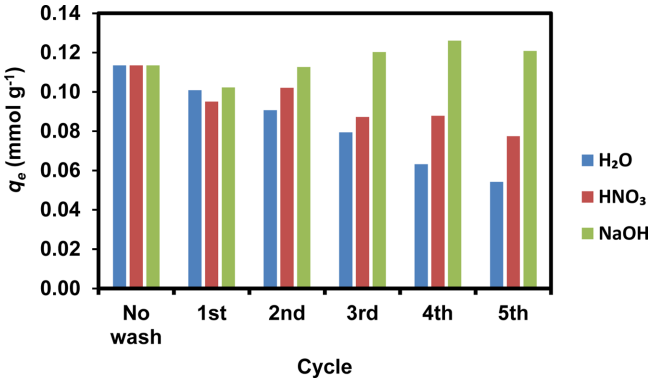

Fig. 10. The adsorption capacity of CDP after number of regeneration cycle.

Positive ΔS^o value suggests a random and disorderly increase at the biosorbent-adsorbate interface with possible structural changes[16].

3-8. Regeneration study

Reusability of a material is highly sought in practical applications as it would greatly reduce the cost of using new batch of the same material. Fig. 10 shows the performance of CDP within five cycles of regeneration study. Washing with distilled water was not able to regenerate CDP ability to adsorb MV as a fresh sample. Although washing with 0.1 M HNO_3 produced a better result, the adsorption capacity of CDP decreased throughout the cycles. 0.1 M NaOH was not only able to regenerate CDP ability to adsorb MV but it also improved the adsorption capacity of CDP from 0.1134 mmol g^{-1} in fresh sample to 0.1202 mmol g^{-1} in the 5th cycle. Removal of surface impurities can be achieved by acid and/or alkali treatment which improves surface roughness and opening the reactive functional groups on the surface such as OH and it was reported that many biosorbents' adsorption capacities can be enhanced by treating them with acid and base[54-56]. NaOH can reveal the reactive functional as it is known to remove fats, waxes and low molecular weight lignin[57]. Thus, it is possible that CDP's surface was modified when base was used to remove MV.

4. Conclusion

Cempedak Durian peel (CDP), a waste material, demonstrates remarkable ability for removal of methyl violet (MV) dye from aqueous solution with an adsorption capacity of 238 mg g^{-1} according to the Langmuir adsorption model, which is the best fitted model compared to the other models investigated: Freundlich and Redlich Peterson. The adsorption of MV on CDP takes place at a fairly fast rate, reaching equilibrium within 60 min. The adsorption reaction of MV on CDP is endothermic and spontaneous. The presence of cationic species hinders the adsorption of cationic MV species being adsorbed, and furthermore, K, Ca and Mg ion contents in the CDP matrix are found to be decreased upon treatment with CDP according to XRF spectroscopic information, demonstrating the interaction between metal ions and MV species. Further, CDP can be successfully regenerated

using 0.1 M NaOH where the adsorption capacity increases throughout the cycles.

Acknowledgement

The authors are grateful to the Government of Brunei Darussalam and the Universiti Brunei Darussalam for their financial support. The authors would like to thank the Centre of Advanced Material and Energy Science (CAMES) Group and the Department of Biology at UBD for the use of SEM and XRF.

References

1. Aksu, Z., *Process Biochem.*, **40**, 997(2005).
2. Rahchamani, J., Mousavi, H. Z. and Behzad, M., *Desalination*, **267**, 256(2011).
3. Sivakumar, R. S., Senthilkumar, P. and Subburam, V., *Bioresour. Technol.*, **80**, 233-235(2001).
4. Abdolali, A., Guo, W. S., Ngo, H. H., Chen, S. S., Nguyen, N. C. and Tung, K. L., *Bioresour. Technol.*, **160**, 57(2014).
5. Deniz, F., Karaman, S. and Saygideger, S. D., *Desalination*, **270**, 199(2011).
6. Dahri, M. K., Kooh, M. R. R. and Lim, L. B. L., *ISRN Environ. Chem.*, **2013**, (2013).
7. Chieng, H. I., Lim, L. B. L. and Priyantha, N., *J. Appl. Sci. Environ. Sanitat.*, **8**, 303(2013).
8. Chieng, H. I., Zehra, T., Lim, L. B. L., Priyantha, N. and Tennakoon, D. T. B., *Environ. Earth. Sci.*, **72**, 2263(2014).
9. Zehra, T., Priyantha, N., Lim, L. B. L. and Iqbal, E., *Desalin. Water Treat.*, 1(2014).
10. Chieng, H. I., Lim, L. B. L. and Priyantha, N., *Desalin. Water Treat.*, 1(2014).
11. Wu, Y., Mi, X., Jiang, L., Li, B. and Feng, S., *Korean J. Chem. Eng.*, **28**, 895(2011).
12. Rehman, M. S. U., Munir, M., Ashfaq, M., Rashid, N., Nazar, M. F., Danish, M. and Han, J.-I., *Chem. Eng. J.*, **228**, 54(2013).
13. Lim, L. B. L., Priyantha, N., Chan, C. M., Matassan, D., Chieng, H. I. and Kooh, M. R. R., *Arab. J. Sci. Eng.*, **39**, 6757(2014).
14. Rajaram, R., Banu, J. S. and Mathivanan, K., *Toxicol. Environ. Chem.*, **95**, 590(2013).
15. Mao, J., Won, S., Min, J. and Yun, Y.-S., *Korean J. Chem. Eng.*, **25**, 1060(2008).
16. Priyantha, N., Lim, L. B. L., Dahri, M. K. and Tennakoon, D. T. B., *J. Appl. Sci. Environ. Sanitat.*, **8**, 179(2013).
17. Bhatti, H., Bajwa, I., Hanif, M. and Bukhari, I., *Korean J. Chem. Eng.*, **27**, 218(2010).
18. Lim, L. B. L., Priyantha, N., Ramli, U. K. and Chieng, H. I., *J. Appl. Phytotechnol. Environ. Sanitat.*, **3**, 65(2014).
19. Lafi, R., ben Fradj, A., Hafiane, A. and Hameed, B. H., *Korean J. Chem. Eng.*, **31**, 2198(2014).
20. Keshtkar, A. and Hassani, M., *Korean J. Chem. Eng.*, **31**, 289 (2014).
21. Lee, H. and Suh, J., *Korean J. Chem. Eng.*, **17**, 477(2000).
22. Lillie, R. D. and Conn, H. J., *Conn's Biological Stains: a Handbook on the Nature and Uses of the Dyes Employed in the Biological Laboratory*, Williams & Wilkins, Baltimore(1977).
23. Hameed, B. H., *Journal of Hazardous Materials*, **154**, 204 (2008).
24. Slokar, Y. M., Majcen Le, and Marechal, A., *Dyes Pigments*, **37**, 335(1998).
25. Vachálková, A., Novotný, L. and Blesová, M., *Neoplasma*, **43**, 113(1996).
26. Tang, Y. P., Lim, L. B. L. and Wimmer, F. L., *Int. Food. Res. J.*, **20**, 409 (2013).
27. Lim, L. B. L., Chieng, H. I. and Wimmer, F. L., *ASEAN J. Sci. Technol. Dev.*, **28**, 122(2011).
28. Lim, L. B. L., Priyantha, N., Ing, C. H., Dahri, M. K., Tennakoon, D. T. B., Zehra, T. and Suklueng, M., *Desalin. Water Treat.*, 1(2013).
29. Chieng, H. I., Lim, L. B. L. and Priyantha, N., *Environ. Technol.*, **36**, 86(2014).
30. Lim, L. B. L., Priyantha, N., Tennakoon, D. T. B. and Dahri, M. K., *Envion. Sci. Pollut. Res.*, **19**, 3250(2012).
31. Shawabkeh, R., Al-Khashman, O., Al-Omari, H. and Shawabkeh, A., *Environmentalist*, **27**, 357-363(2007).
32. Ghaedi, M., Hossainian, H., Montazerozohori, M., Shokrollahi, A., Shojaipour, F., Soylak, M. and Purkait, M. K., *Desalination*, **281**, 226(2011).
33. Langmuir, I., *J. Am. Chem. Soc.*, **40**, 1361(1918).
34. Freundlich, H. M. F., *J. Phys. Chem.*, **57**, 385(1906).
35. Redlich, O. and Peterson, D. L., *J. Phys. Chem.*, **63**, 1024 (1959).
36. Tsai, S. C. and Juang, K. W., *J. Radioanal. Nucl. Chem.*, **243**, 741(2000).
37. Weber, T. W. and Chakravorti, R. K., *J. Amer. Inst. Chem. Engrs.*, **20**, 228(1974).
38. McKay, G., Blair, H. S. and Gardner, J. R., *J. Appl. Polym. Sci.*, **27**, 3043(1982).
39. Annadurai, G., Juang, R. S. and Lee, D. J., *J. Hazard. Mater.*, **92**, 263(2002).
40. Li, P., Su, Y. J., Wang, Y., Liu, B. and Sun, L. M., *J. Hazard. Mater.*, **179**, 43(2010).
41. Cengiz, S. and Cavas, L., *Mar. Biotechnol.*, **6**, 728(2010).
42. Duran, C., Ozdes, D., Gundogdu, A. and Senturk, H. B., *J. Chem. Eng. Data.*, **56**, 2136(2011).
43. Mane, V. S. and Babu, P. V. V., *Desalination*, **273**, 321(2011).
44. Lagergren, S., *K. Sven. Vetenskapsakad. Handl.*, **24**, 1(1898).
45. Ho, Y. S. and McKay, G., *Process Biochem.*, **34**, 451(1999).
46. Weber, W. and Morris, J., *J. Sanit. Eng. Div.*, **89**, 31(1963).
47. Boyd, G. E., Adamson, A. W. and Myers Jr, L. S., *J. Am. Chem. Soc.*, **69**, 2836(1947).
48. Li, Q., Yue, Q.-Y., Su, Y., Gao, B.-Y. and Fu, L., *J. Hazard. Mater.*, **147**, 370(2007).
49. Akkaya, G. and Özer, A., *Process Biochem.*, **40**, 3559(2005).
50. Gad, H. M. H. and El-Sayed, A. A., *J. Hazard. Mater.*, **168**, 1070(2009).
51. Hu, Y., Guo, T., Ye, X., Li, Q., Guo, M., Liu, H. and Wu, Z., *Chem. Eng. J.*, **228**, 392(2013).
52. Vilar, V. J. P., Botelho, C. M. S. and Boaventura, R. A. R., *Process Biochem.*, **40**, 3267(2005).
53. Newcombe, G. and Drikas, M., *Carbon*, **35**, 1239(1997).
54. Abdallah, R. and Taha, S., *Chem. Eng. J.*, **195**, 69(2012).
55. Kumar, D. and Gaur, J. P., *Bioresour. Technol.*, **102**, 2529 (2011).
56. Fernandez, M. E., Nunell, G. V., Bonelli, P. R. and Cukierman, A. L., *Bioresour. Technol.*, **106**, 55(2012).
57. Chowdhury, S., Misra, R., Kushwaha, P. and Das, P., *Biorem. J.*, **15**, 77(2011).